

Analysis of BRDF and Albedo Properties of Pure and Mixed Surface Types From Terra MISR Using Landsat High-Resolution Land Cover and Angular Unmixing Technique

*K.Khlopenkov and A.P. Trishchenko,
Canada Centre for Remote Sensing
Ottawa, Ontario, Canada;*

*Y. Luo
Noetix Research Inc.
Ottawa, Ontario, Canada*

Introduction

The bi-directional reflectance distribution function (BRDF) determines the degree of anisotropy of the surface's reflective properties (Nicodemus et al. 1977). This is a basic parameter employed in the vegetation structure retrievals and characterization of surface albedo. An important feature of the BRDF shape is the amplitude and width of the hot spot and dark spot areas in the principal plane direction. The general BRDF shape in the direction of the perpendicular plane is also important. Retrieving the BRDF shape from a satellite observation is a difficult task (Luo et al. 2004). In general, satellite sensors do not provide simultaneous measurements of reflectance in all viewing directions. For example, in BRDF retrievals from moderate-resolution imaging spectroradiometer (MODIS) observations (Schaaf et al. 2002), angular coverage is achieved by assembling clear-sky pixels from different orbits within a certain interval of time: 8, 10, or 16 days. Multiangular observations from multi-angle imaging spectrometer (MISR) contain simultaneous measurements at nine viewing directions, thus providing much better capabilities for surface BRDF retrievals and an atmospheric correction for the presence of the atmospheric aerosols. However, since MISR has a narrow swath and operates on sun-synchronous orbit, it cannot provide complete coverage of the entire angular domain (Luo et al. 2004). Therefore, it is important to have the BRDF models for generic landcover types, which will be adjusted for each particular case, based on a limited sampling of the angular measurements.

To construct the generic BRDF for a specific landcover type, one needs to ensure an adequate sampling of observations in the viewing zenith angle vs. relative azimuth angle (VZA-RAA) plane for various ranges of the solar zenith angle (SZA). The best strategy to achieve this task is to collect all of the reflectance data for all of the pixels with the same landcover type, and then use these data to derive the generic BRDF shape (Luo et al. 2004). In reality, however, the definition of landcover type may not be a perfect identification of the type of surface element, from the BRDF point of view. For example, "cropland" is a frequently used landcover type to denote a large variety of vegetation types, such as wheat, corn, soybeans, and many others. Depending on the season, the area identified as cropland may correspond also to baresoil or the mixed conditions – baresoil and vegetation. Another problem is

related to the mixing of various landcover types within one pixel. If the pixel size is larger than the typical size of agricultural fields, then the pixel contains a mixture of various fields. Also, there is a problem associated with similar landcover types in different conditions and/or stages of growth. Although identical in the landcover type, their BRDF properties may look very different.

Below, we present some of the results of our analysis aimed at studying the problem of the mixing of various landcover types and its effect on the BRDF at a coarse spatial resolution. In particular, we analyzed MISR observations and deduced the BRDFs for pure landcover types using the angular unmixing method. We also studied the relationship between the BRDF shape of the mixed landcover classes and the level of the Normalized Difference Vegetation Index (NDVI).

Angular Unmixing Method

The area of interest encompasses the region of approximately $20 \times 20 \text{ km}^2$ around the Atmospheric Radiation Measurement (ARM) Program Southern Great Plains (SGP) Central Facility (CF) located in Northern Oklahoma, USA. LANDSAT data were used to produce landcover maps with 30m spatial resolution. At this spatial resolution, the majority of pixels correspond to the pure landcover types (such as wheat, grass, baresoil, etc.). The digital landcover map was created first by conducting an unsupervised classification for a large number of classes. The classes were then aggregated to a smaller number of landcover types using the results of the ground survey. An example of the landcover map derived from LANDSAT is shown in Figure 1. The map corresponds to the mid-May conditions in 2003. Its accuracy is estimated to be better than 95%.

The MODIS and MISR images are used to produce surface BRDF/Albedo on regular basis (Schaaf et al. 2002; Diner et al. 1999). The typical spatial resolution for MISR product is 1.1 km. Unlike LANDSAT, almost all of the pixels in the MISR product for the area shown in Figure 1 represent mixed landcover types. The rectangular grid on Figure 1 denotes the location of pixels from the MISR Level-2 surface product (version 15).

The hemispheric backscattering albedo of the atmosphere under clear sky conditions is very small, and one can neglect the effects of multiple scattering of the surface reflected radiation (the adjacency effect). With this assumption, the total radiation reflected from a coarse resolution pixel can be considered as a linear integral over the subpixels. Therefore, the reflectance R of a pixel i containing a mixture of landcover types can be represented as a linear superposition of reflectances r_c for each landcover class c :

$$R_i(\theta_0, \theta, \phi, \lambda) = \sum_c w_{c,i} r_c(\theta_0, \theta, \phi, \lambda), \quad (1)$$

where θ_0, θ are the sun and view zenith angles, ϕ is the relative azimuth angle, λ is the wavelength or spectral band, and $w_{c,i}$ is the weight of each class, i.e., the fractional coverage of the landcover class c for pixel i , with $\sum_c w_c = 1$. LANDSAT-derived map was used to obtain the weights w_c .

For our analysis, we initially selected five distinct landcover classes present in the ARM SGP area: wheat, grass, baresoil, trees/shrubs, and water. To reduce the impact of low-scale variability, we

analyzed data by grouping several coarse resolution pixels together. Taking a group of MISR pixels and writing Equation 1 for each pixel, a set of linear equations was built with the five unknowns, r_c , being the average reflectances of each landcover class. The solution was derived using a least-squares fit since the number of unknowns was less than the number of equations. To reduce the noise and still produce enough data for building reliable statistics, we used groups ranging from 12 to 16 pixels. Since the trees/shrubs and water landcover classes have typically a very low abundance in the SGP area, the retrievals for these classes contain a high level of noise. As such, they were excluded from the subsequent analysis.

Obtained results and discussion

The MISR dataset contains several layers of data. We used the Bidirectional Reflectance Factor (BRF), defined as the surface-leaving radiance divided by the radiance from a lambertian reflector illuminated from a single direction. The BRF layer contains data images with 1.1km per pixel spatial resolution where each pixel has values of reflectance measured from nine different directions (with negligible time lag) in four spectral channels (Diner et al. 1999).

The application of the unmixing method is possible for the multiangular MISR data, but the routine has to be applied to each viewing angle independently. Considering one spectral channel and one direction (described by the view angle θ and the relative azimuth angle ϕ), we can write Equation 1 for the reflectance of each MISR pixel. Combining several pixels in one group, and solving the overdetermined set of linear equations, we can obtain the least-squares solution for the characteristic reflectances of each landcover class. Repeating the procedure for each direction, we can collect nine values of reflectance for each group of pixels.

It is also possible to use more than one MISR orbit over the region of interest in order to collect more values of directional reflectance measured at different directions. The data must be taken within short period of time and correspond to cloud-free conditions. In the case of the May 2003 data series, only one satellite pass was available, whereas in case of September 2002, it was possible to use two passes within a nine-day interval.

Having collected several values of directional reflectance for each landcover class, it is possible to fit a BRDF model to these data. We limited our analysis to two BRDF models: the RossThick–LiSparse model (Wanner et al. 1995), and the modified Rahman model (Rahman et al. 1993), employed in the MISR data processing, as defined by Equation 2:

$$\begin{aligned}
R(\theta_0, \theta, \phi) &= r_0 (\cos \theta \cos \theta_0 (\cos \theta + \cos \theta_0))^{k-1} h \exp(-b \cos \xi) \\
h(\theta_0, \theta, \phi) &= 1 + \frac{1 - r_0}{1 + G(\theta_0, \theta, \phi)} \\
G(\theta_0, \theta, \phi) &= \sqrt{\tan^2 \theta + \tan^2 \theta_0 - 2 \tan \theta \tan \theta_0 \cos \phi} \\
\cos \xi &= \cos \theta \cos \theta_0 + \sin \theta \sin \theta_0 \cos \phi
\end{aligned} \tag{2}$$

where r_0 , k , and b are the three fitting parameters of the model, responsible for the amplitude of the BRDF, its overall shape and the hot spot area, respectively.

The obtained sets of multiangular data were fitted using the Levenberg-Marquardt method (Press et al. 1992) of non-linear least-squares fitting of multi-dimensional functions. Figure 2 presents the comparison of the fitted models with the observed multi-angular reflectances for selected MISR pixels that represent pure landcover classes. It should be noted that the MISR measurements do not lie in the principal plane, but at about 45° relative to the principal plane. For this reason, the hot spot area ($\theta_0 = 23.5^\circ$ for this case) is not well defined.

For each pixel group, we obtained three model parameters r_0 , k , and b for each landcover class. The fitting procedure was applied to each pixel group with different fractional coverage of the landcover classes. The results of the fitting for the red MISR channel (672 nm) are shown in Figure 3. Each panel on Figure 3 shows the parameter derived for each landcover class for all pixel groups. The horizontal axes show the fractional coverage of a particular class within the pixel group. For example, x values close to 1.0 correspond to pixels with a pure landcover type. It is seen that the scattering of the parameters becomes smaller when the fractional coverage is higher. Larger scattering for small fractional coverage probably occurs due to small-scale surface inhomogeneities and uncertainties in image registration for the coarse resolution pixel, when an insignificant mismatch in the pixel location has a large impact on the small fraction of the area. The smallest scattering is achieved for the wheat landcover type for all three model parameters. A larger scattering is observed for the grass landcover type, which can presumably be explained by the higher variability in the reflective properties for grass fields. The largest scattering of the retrieval results is observed for the baresoil landcover type. This may be attributed to the high variability of the reflectance for this landcover class, which in many cases can be a mixture of dry grass, corn stalks, and open soil. Another contributing factor is the low abundance of this class in the spring season. This is confirmed by the results of the analysis for the Fall 2002, when baresoil, which replaces the wheat fields, becomes a dominant class.

A similar set of graphs for the near infrared (NIR) channel (866 nm) is shown in Figure 4.

The relationship between the BRDF model parameters and the NDVI index for pure MISR pixels is presented in Figure 5. Analysis of BRDF parameters against the NDVI suggests that the NDVI index has the most significant impact on the overall amplitude of the reflectance. The anisotropy parameters, geometric f_{GEO} and volumetric f_{VOL} parameters of the Ross-Li and k and b parameters of the modified Rahman model, show a relatively weak correlation with NDVI for the considered landcover types and scenes.

Conclusion

A high-spatial resolution landcover map of the agricultural area in the ARM SGP area was produced from LANDSAT data and was used to study the BRDF properties of pure and mixed landcover types employing the MISR data. Two BRDF models were used: the Ross-Li model and the modified Rahman model. Neglecting the adjacency effect at 1km scale, we assumed the linear mixing model, which can be inverted using least-squares fitting.

In general, our approach produces results consistent with independent analysis based on ground observations. The angular unmixing method can be applied to deduce the BRDF properties of the pure landcover classes. The uncertainty of this approach becomes smaller when the fractional area or the particular class increases.

In case of the NIR channel, the k -parameter is higher for wheat than for grass, while in the visible red channels, the picture is reversed. In general, the variability of the retrieved parameters for wheat is lower, and for baresoil, it is the highest. The latter is especially true when this class represents low fractional coverage.

Analysis of BRDF parameters against the NDVI shows that the considered landcover classes are mostly distinguished by their spectral signatures, rather than by the anisotropy properties. This suggests that the NDVI can be used as the parameter for the separation/aggregation of pixels in the BRDF fitting procedure independent on the specific type of vegetation (grass, wheat, soil, or mixture of the above), since it affects mostly the amplitude but not the shape of the BRDF for cropland types.

Acknowledgement

This research was supported by the US Department of Energy Atmospheric Radiation Measurement Program under grant No. DE-FG02-02ER63351.

Corresponding Author

Alexander P. Trishchenko, trichtch@ccrs.nrcan.gc.ca, (613) 995-5787

References

- Nicodemus, F. E., J. C. Richmond, J. J. Hsia, I. Ginsberg, and T. Limperis, 1997: *Geometric considerations and nomenclature for reflectance*. U. S. Dept. of Commerce, NBS Monograph.
- Luo, Y., A. P. Trishchenko, R. Latifovic, and Z. Li, 2004: Surface bidirectional reflectance and albedo properties derived by a landcover based approach from the MODIS observations, *J. Geophys. Res. submitted*.
- Schaaf, C. B., F. Gao, A. H. Strahler, W. Lucht, X. Li, T. Tsang, N. C. Strugnell, X. Zhang, Y. Jin, J.-P. Muller, P. Lewis, M. Barnsley, P. Hobson, M. Disney, G. Roberts, M. Dunderdale, C. Doll, R. d'Entremont, B. Hu, S. Liang, and J. L. Privette, 2002: First operational BRDF, albedo and nadir reflectance products from MODIS, *Remote Sens. Environ.*, 83, 135–148.
- Diner, D. J., J. V. Martonchik, C. Borel, S. A. W. Gerstl, H. R. Gordon, Y. Knyazikhin, R. Myneni, B. Pinty, and M. Verstraete, 1999: MISR level 2 surface retrieval, *Report of JPL D-11401*, (http://eospso.gsfc.nasa.gov/eos_homepage/for_scientists/atbd/docs/MISR/atbd-misr-10.pdf).

- Wanner, W., X. Li, and A. H. Strahler, 1995: On the derivation of kernels for kernel-driven models of bi-directional reflectance *J. Geophys. Res.*, 100, 21077–21090.
- Rahman, H., B. Pinty, and M. Verstraete, 1993: Coupled surface atmosphere reflectance (CSAR) model, 2, Semiempirical surface model usable with NOAA Advanced Very High Resolution Radiometer data, *J. Geophys. Res.*, 98, 20,791–20,801.
- Press, W.H., S.A. Teukolsky, W.T. Vetterling, and B.P. Flannery, 1992: *Numerical Recipes in FORTRAN: The Art of Scientific Computing*, 2nd Ed., Cambridge University Press, Cambridge, 675–683.

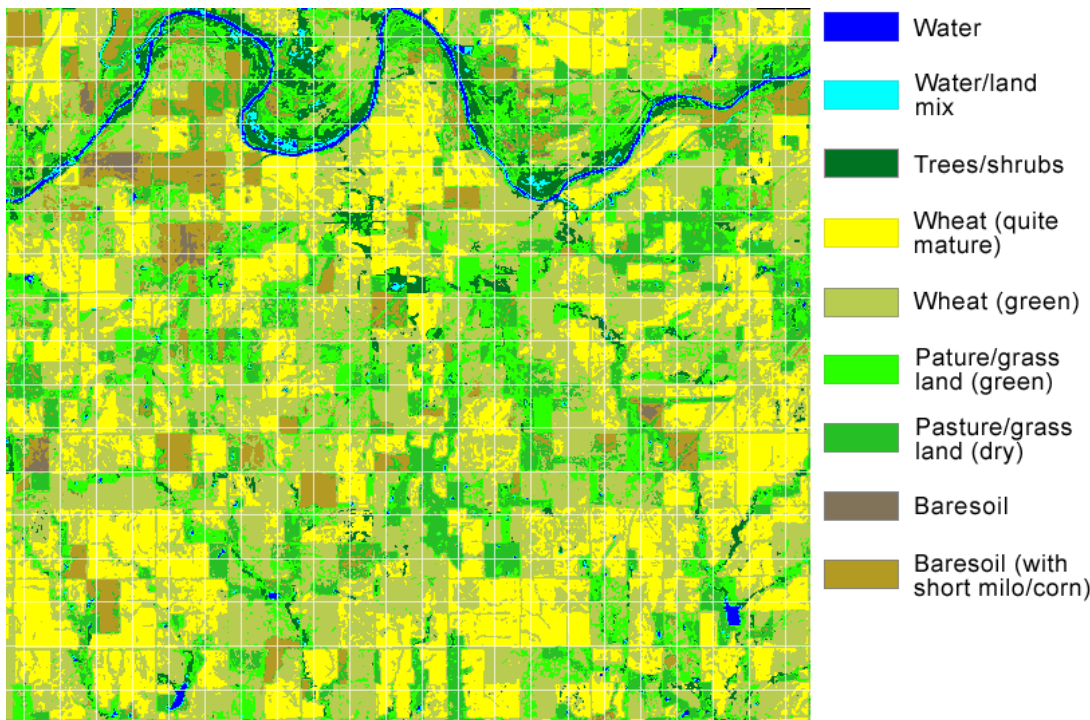


Figure 1. Example of the landcover map for SGP area derived from a LANDSAT TM image and ground survey. The rectangular grid shows the location of MISR pixels.

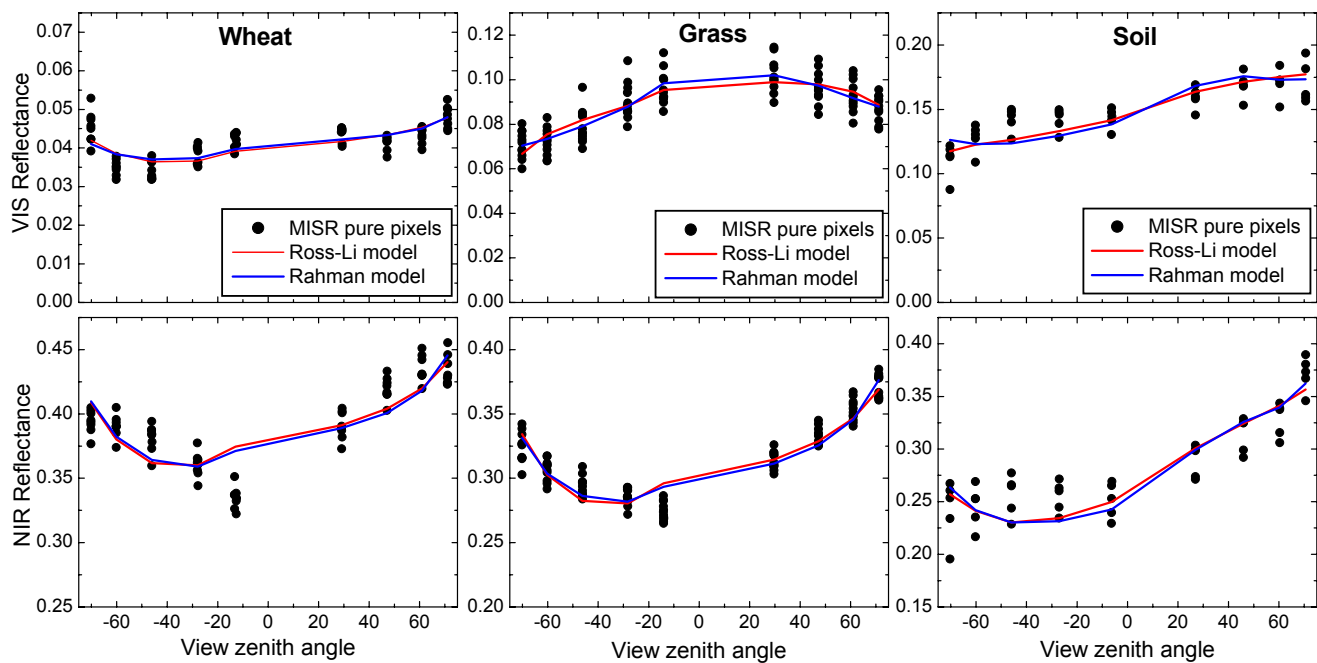


Figure 2. Fitting the MISR reflectances with the Ross-Li and modified Rahman models for the pixels with pure landcover types: grass, wheat, soil.

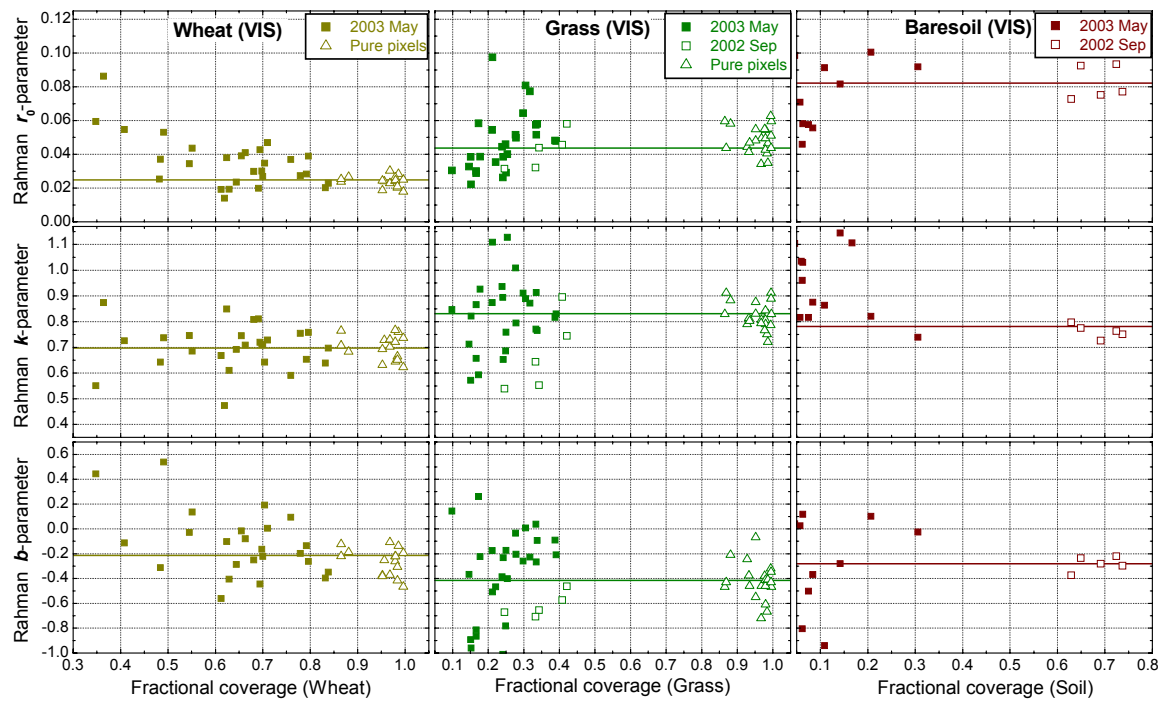


Figure 3. Rahman model parameters for the red spectral band. Data for MISR pixels with low fractional coverage are shown as squares. Pure pixels are shown as triangles. Solid lines show the weighed average values for pure pixels.

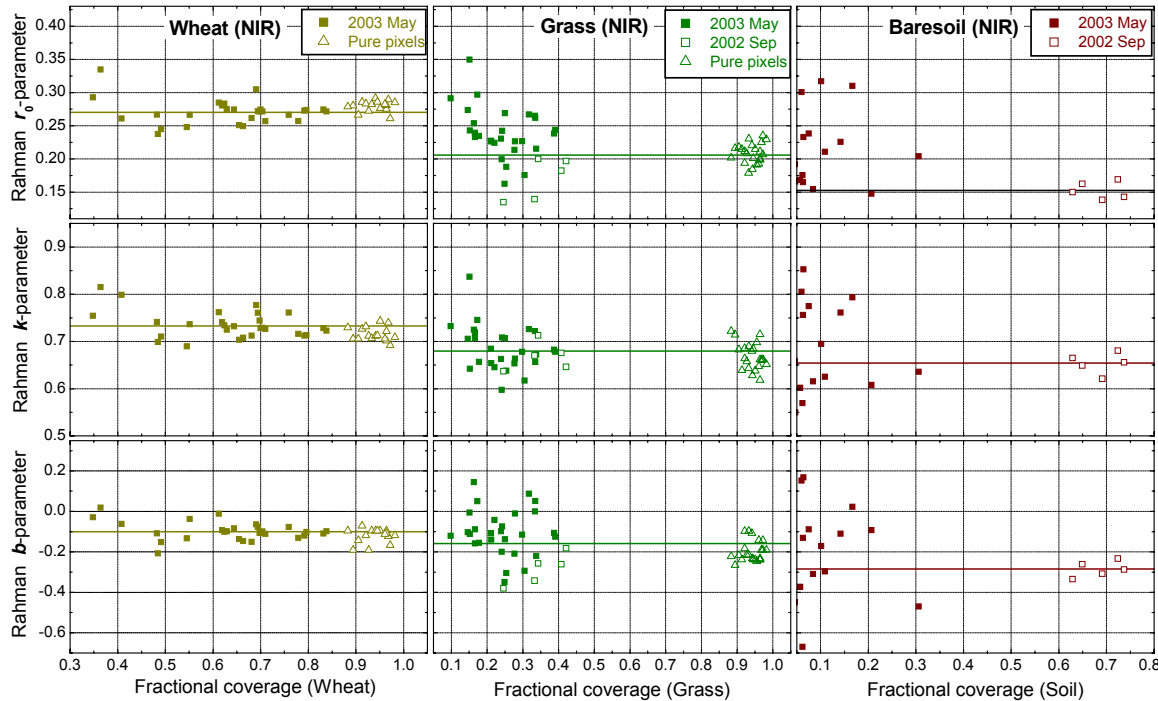


Figure 4. Same as in Figure 3, but for the NIR channel.

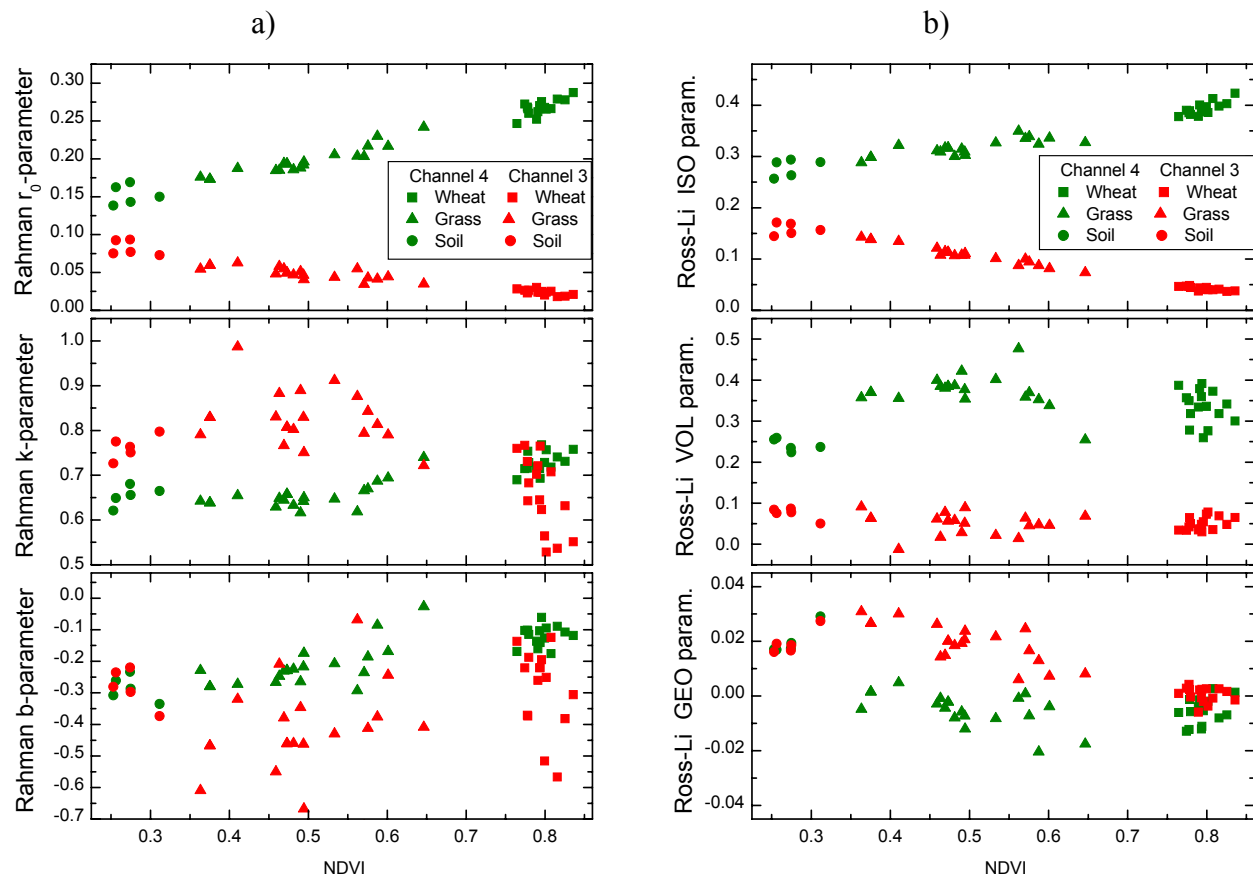


Figure 5. Comparison of fitted model parameters with the NDVI for pure MISR pixels for ch.3 (red) and ch.4 (NIR). Unconstrained fitting leads to negative fGEO .